

EXOTIC SEARCHES AT ATLAS

D.M. GINGRICH

(on behalf of the ATLAS Collaboration)

*Centre for Particle Physics, Department of Physics, University of Alberta,
Edmonton, AB T6G 2G7 Canada &
TRIUMF, Vancouver, BC V6T 2A3 Canada*

We present the first results of searches for new physics with the ATLAS detector using the 2010 Large Hadron Collider proton-proton collision data at a centre of mass energy of 7 TeV. After a few months of operation, these searches already go beyond the reach of previous experiments, and start to explore new territories.

1 Introduction

This paper presents five searches for new physics in proton-proton collisions using the ATLAS detector at the Large Hadron Collider. The data were collected in 2010 at a centre of mass energy of 7 TeV. The first two searches use 3.1 pb^{-1} of early data, while the later three searches use the full 2010 data set with a typical luminosity of 36 pb^{-1} .

2 Long-Lived Highly Ionising Particles

The ATLAS collaboration has performed a search for massive long-lived highly ionising particles (HIP).¹ Some examples that may give rise to highly ionising particle signatures are Q-balls, black hole remnants, magnetic monopoles, and dyons. We have performed a model independent search. Due to their large mass, HIPs are also characterised by their non-relativistic speeds, as well as, high electric charge. We expect large amounts of energy loss through ionisation for these states. In ATLAS, HIPs would leave tracks in the inner tracking detector, matched to narrow energy loss in the electromagnetic calorimeter.

ATLAS is not able to search for HIP of all charges, masses, and lifetimes. The accessible parameter space was determined as follows. A lower charge bound of $|q| \geq 6e$ was determined by the $E_T > 10 \text{ GeV}$ trigger threshold. The upper charge bound of $|q| \leq 17e$ was determined by delta electrons and electron recombination. An upper bound on the mass of 1 TeV was determined by trigger timing constraints. A lifetime greater than 100 ns was required to maintain narrow energy deposits. A data sample with a luminosity of 3.1 pb^{-1} was used.

HIPs were discriminated by the proportion of high-ionisation hits and the lateral extent of the energy deposition. Specifically, the fraction f_{HT} of transition radiation tracker (TRT) hits on the track which pass a high ionisation threshold was used. In addition, a requirement on the fraction of energy outside the three most energetic cells associated to a selected electromagnetic (EM) energy cluster, in the second EM calorimeter layer, w_2 , was made. Figure 1 shows that the

data matches Standard Model (SM) expectations, and no HIPs were observed. The estimated background in the signal region was 0.019 ± 0.005 events. Limits for particles produced in the acceptance kinematic region and by Drell-Yan production are shown in Table 1. A Bayesian statistical approach with a uniform prior for the signal was used. HIP masses above 800 GeV are probed for the first time at particle colliders.

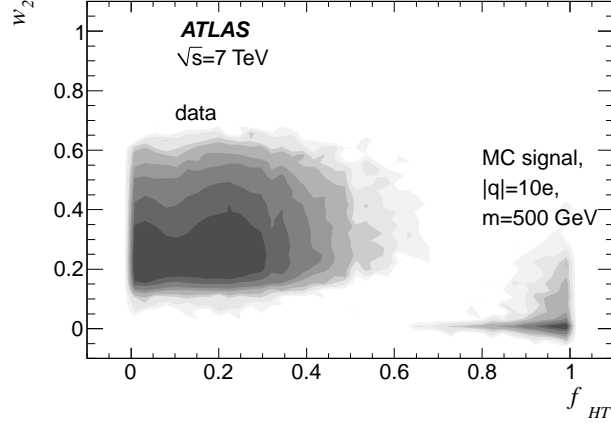


Figure 1: Contours of w_2 versus f_{HT} distributions showing the density of entries on a log scale. Data and a signal Monte Carlo simulated sample are shown.

Table 1: Inclusive and pair production cross section upper limits (95% C.L.) for long-lived massive particles with high electric charges $|q|$, produced in the search acceptance and assuming a Drell-Yan production mechanism.

Mass	Inclusive Search			Drell-Yan Mechanism		
	$ q = 6e$	$ q = 10e$	$ q = 17e$	$ q = 6e$	$ q = 10e$	$ q = 17e$
200 GeV	1.4 pb	1.2 pb	2.1 pb	11.5 pb	5.9 pb	9.1 pb
500 GeV	1.2 pb	1.2 pb	1.6 pb	7.2 pb	4.3 pb	5.3 pb
1000 GeV	2.2 pb	1.2 pb	1.5 pb	9.3 pb	3.4 pb	4.3 pb

3 Diphoton with Large Missing Energy

ATLAS has performed a search for events with diphotons ($\gamma\gamma$) and large missing transverse energy E_T^{miss} .² This signature has been interpreted in the context of Universal Extra Dimensions (UED). We considered a single TeV^{-1} sized UED with a compactification radius R . In this model, the lightest Kaluza-Klein (KK) particle (LKP) is the KK photon γ^* . The KK particles are produced as pairs of KK quarks and/or KK gluons in the strong interaction. These KK particles then decay down, via KK states, to the LKP. The LKP decays by $\gamma^* \rightarrow \gamma + G$. We interpreted the results of the search using a model in which $\Lambda R = 20$, where Λ is the UV cutoff and R is a free parameter

Figure 2 shows the E_T^{miss} spectrum of events with diphotons. Events were required to have two photons each with $E_T > 25$ GeV, and an event $E_T^{\text{miss}} > 75$ GeV. Zero signal events were observed and the estimated background was $0.32 \pm 0.16_{-0.10}^{+0.37}$ events. Figure 3 shows upper limits on the cross section. The upper limits were calculated using a Bayesian approach with a flat prior for the signal cross section. It was verified that the result is not very sensitive to the detailed form of the assumed prior. In context of the previously specified model, values of $1/R < 728$ GeV are excluded. This is the most sensitive limit on this model to date.

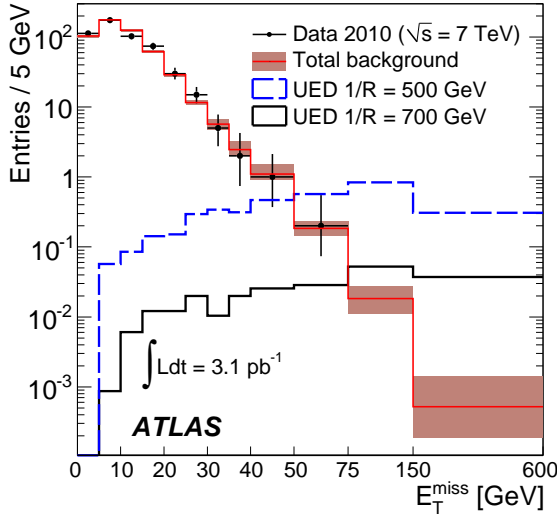


Figure 2: E_T^{miss} spectra for $\gamma\gamma$ events, compared to the total SM background as estimated from data. Also shown are two hypothetical UED signals. The vertical error bars and shaded bands show the statistical errors.

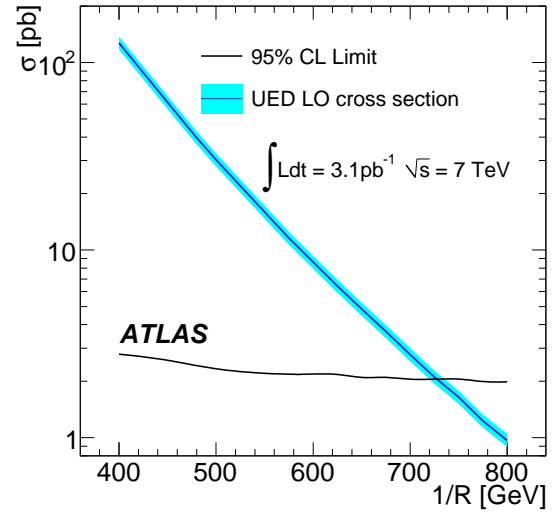


Figure 3: 95% C.L. upper limits on the UED production cross section, and the leading order (LO) theory cross section prediction, as a function of $1/R$. The shaded band shows the PDF uncertainty.

4 Search for New Physics in Dijets

ATLAS has performed a study of dijet events using both the invariant mass of the two jets and angular distributions of energetic jets up to 3.5 TeV.³ For the invariant mass studies, we required $p_T^j > 150$ GeV and $p_T^j > 30$ GeV, as well as, $|\Delta\eta_{jj}| > 1.3$. Figure 4 shows that the invariant mass distribution is smooth as expected for QCD jet production and agrees with the SM background parameterisation.

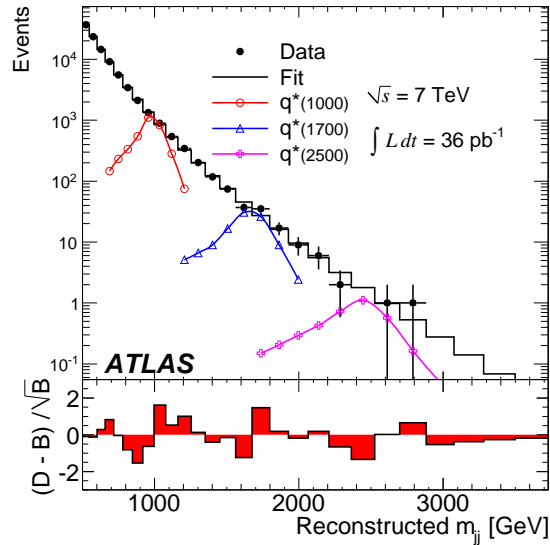


Figure 4: Observed (D) dijet mass distribution (solid dots) fitted using a binned QCD background (B) parameterisation (histogram). Predicted q^* signals normalised to 36 pb^{-1} for masses of 1.0, 1.7, and 2.5 TeV are overlaid. The bin-by-bin significance of the data-background difference is shown in the lower panel.

For the angular distributions, we required $p_T^{j_1} > 60$ GeV and $p_T^{j_2} > 30$ GeV. The rapidities of the two leading jets per event are required to satisfy $y_B = 0.5(y_1 + y_2) < 1.10$ and $y^* = 0.5(y_1 - y_2) < 1.70$. Figure 5 shows the χ distributions, where $\chi = \exp(|y_1 - y_2|) = \exp(2|y^*|)$. Data are consistent with QCD. We also examined the dijet centrality, where $F_\chi(m_{jj}) = N_{\text{events}}(|y^*| < 0.6)/N_{\text{events}}(|y^*| < 1.7)$. This distribution is shown in Fig. 6.

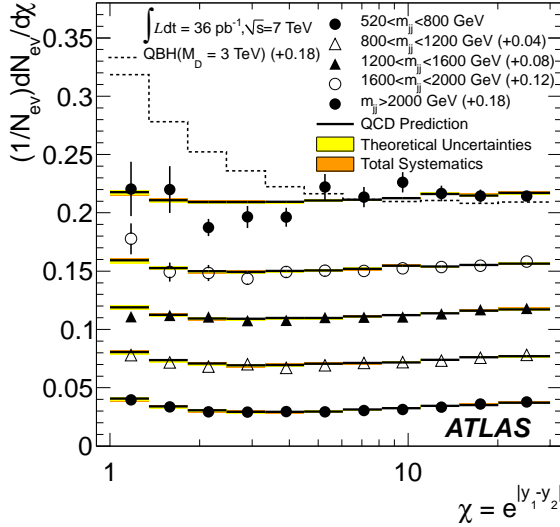


Figure 5: χ distributions for different m_{jj} bins. Shown are the QCD predictions with systematic uncertainties, and data points with statistical uncertainties. The dashed line is the prediction of a quantum black hole (QBH) signal in the highest mass bin. The distributions and QCD predictions have been offset.

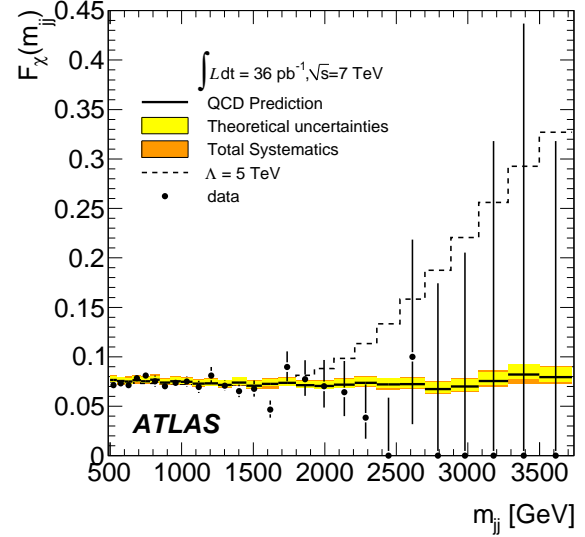


Figure 6: $F_\chi(m_{jj})$ function versus m_{jj} . We show the QCD prediction with systematic uncertainties (band) and data (solid dots) with statistical uncertainties. The expected signal for QCD plus a quark contact interaction with $\Lambda = 0.5$ TeV is also shown.

We now interpret the results using several models, showing both the dijet mass and angular distribution results. For the resonance results, we set Bayesian credibility levels by defining a posterior probability density from the likelihood function for the observed mass spectrum, obtained by a fit to the background functional form and a signal shape derived from MC calculation. For the angular distribution results, likelihood ratios for comparing the different hypotheses and parameter estimators were used. Confidence level limits are set using the frequentist CLs+b approach.

Excited quarks can be produced in $qg \rightarrow q^*$ and decay by $q^* \rightarrow qg, qW/Z/\gamma$. Figure 7 shows the results of the resonance search. Excited quarks are excluded in the mass range $0.60 < m < 2.15$ TeV, while axigluons are excluded in the range $0.60 < m < 2.10$ TeV. Shown in Fig. 8 is the Q distribution, where $Q = -2[\ln(F_\chi(m_{jj})|H0) - \ln(F_\chi(m_{jj})|H1)]$, and $H0$ is the null hypothesis (QCD only) and $H1$ is the hypothesis for new physics. From this analysis, excited quarks in the mass range $0.60 < m < 2.64$ TeV are excluded.

We searched for quantum black holes (QBH) decaying to dijets, where M_D is the higher-dimensional Planck scale and n is the number of extra dimensions. These states would be expected to produce a large mass threshold effect with long tails to higher masses. The results of the resonance search are shown in Fig. 9. Planck scales in the range $0.75 < M_D < 3.67$ TeV are excluded. The results of the angular distributions analysis are shown in Fig. 10. From the $dN/d\chi$ distribution, Planck scales less than 3.69 TeV are excluded, while from the $F_\chi(m_{jj})$ distribution Planck scales of less than 3.78 TeV are excluded.

Finally, limits are given for a generic signal with a Gaussian profile. Signal templates in the range $0.6 < m < 4.0$ with $3\% < \sigma < 15\%$ (5 different σ values) were generated. The results

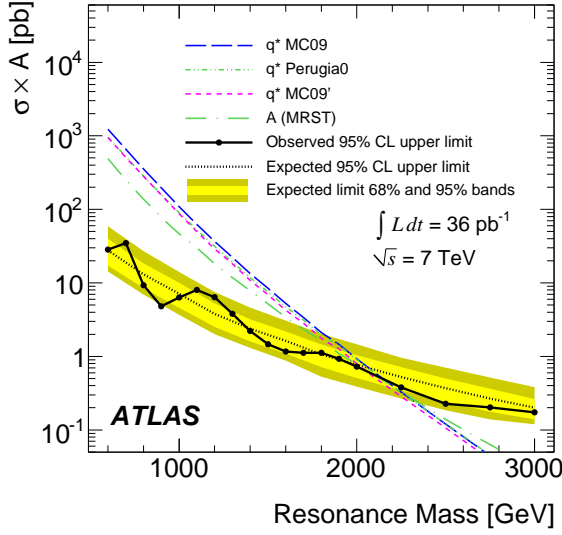


Figure 7: 95% C.L. upper limits on cross section times acceptance for a resonance decaying to dijets taking into account both statistical and systematic uncertainties (points and solid line) compared to an axigluon model and to a q^* model with three alternative MC tunes.

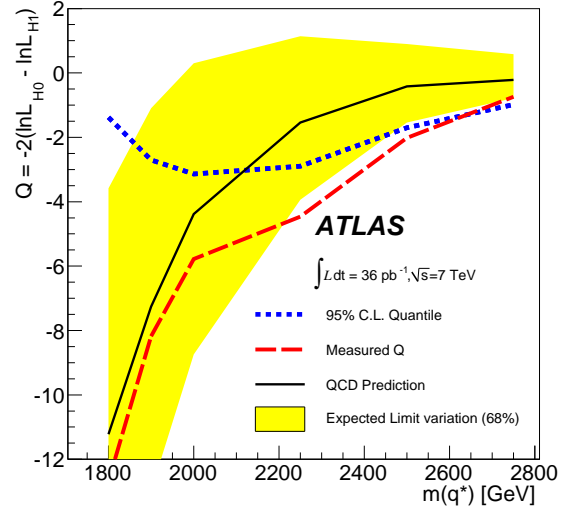


Figure 8: 95% C.L. limits on the excited quark model using the logarithm of the likelihood ratios obtained from the $F_X(m_{jj})$ distributions. The expected 68% interval for the expected limits are shown by the band.

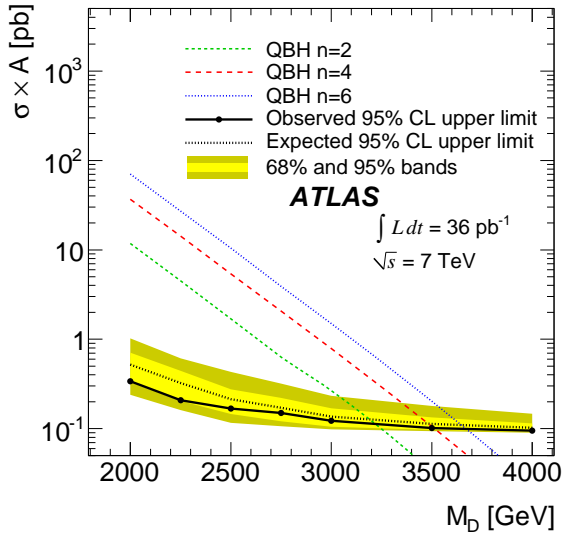


Figure 9: 95% C.L. limits on the cross section times acceptance versus the Planck scale for three quantum black hole (QBH) models, taking into account both statistical and systematic uncertainties.

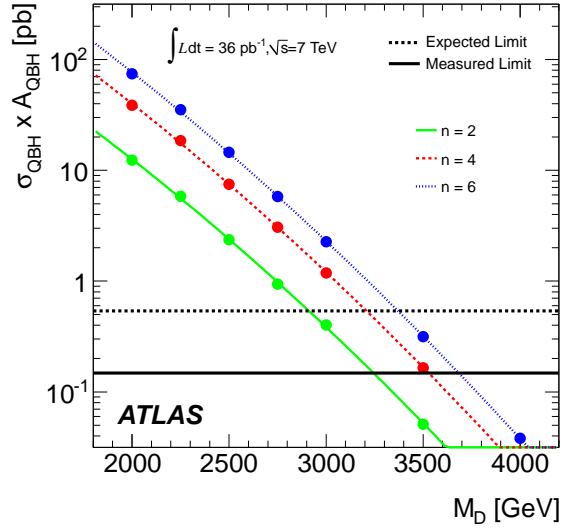


Figure 10: Cross section times acceptance for quantum black holes (QBH) as a function of M_D . The measured and expected limits are shown as the solid and dashed lines.

are shown in Fig. 11. These results can be used for different models by employing the following prescription: 1) Check the validity of the Gaussian signal approximation, and determine the peak and width of the signal; 2) Determine the model acceptance; 3) Calculate the event yield for the model cross section and luminosity of 36 pb^{-1} ; 4) Compare this event yield with the limits in Fig. 11.

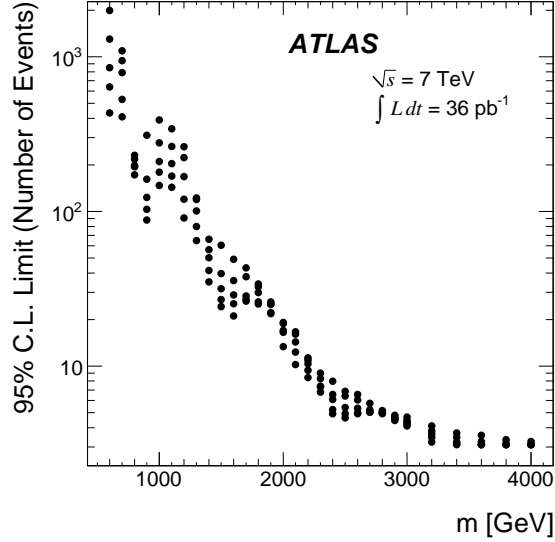


Figure 11: 95% C.L. upper limits for the number of observed events for Gaussians of width σ/m of 0.03, 0.05, 0.07, 0.10, 0.15, at each of various masses m .

5 Lepton plus Missing Transverse Energy

ATLAS has performed a search for high-mass states decaying to an electron or muon with missing energy: $W'/W^* \rightarrow (e/\mu)\nu$.⁴ The W' is a sequential SM boson with the same SM couplings as the W -boson. The W^* is a boson with anomalous magnetic moment type couplings. The search was performed in the transverse mass defined as $m_T = \sqrt{2p_T E_T^{\text{miss}}(1 - \cos \phi_{\ell\nu})}$. Events with electrons were chosen by requiring the electron to have $E_T > 25 \text{ GeV}$, and the event to have $E_T^{\text{miss}} > 25 \text{ GeV}$ and $E_T^{\text{miss}}/E_T > 0.6$. Events with muons were chosen by requiring muons, in the barrel only, to have $p_T > 25 \text{ GeV}$, and the event to have $E_T^{\text{miss}} > 25 \text{ GeV}$. Figure 12 shows the transverse mass distribution for the two channels.

The agreement between data and the expected backgrounds is good. Limits on σB for each W' and W^* mass and decay channel are set using a likelihood function as input to the estimate $CL_s = CL_{s+b}/CL_s$. To set limits, we counted events with $m_T > 0.5 m_{W'/W^*}$. Figure 13 shows the limits on the cross section times branching ratio. A W' with mass below 1.49 TeV and W^* with mass below 1.47 TeV are excluded.

6 High Mass Dilepton Resonances

ATLAS has performed a search for high-mass neutral resonance states decaying to two leptons of the same generation.⁵ Examples of such high-mass resonances are new heavy neutral gauge bosons (Z' and Z^*), the Randall-Sundrum spin-2 graviton, and a spin-1 techni-meson. The search looked for $Z' \rightarrow e^+e^-$ or $\mu^+\mu^-$, where Z' is a high-mass sequential SM (SSM) gauge boson with SM couplings, or a Z' motivated by an E_6 model. Six different E_6 motivated gauge bosons were searched for with different mixing angles between the two $U(1)$ states. We assumed the

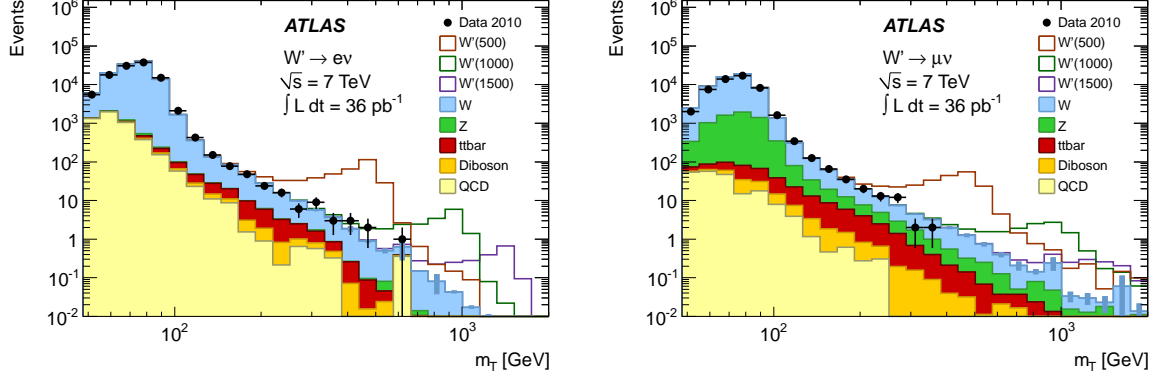


Figure 12: m_T spectra for electron (left) and muon (right) channels after final event selection. The points represent data and the filled histograms show the stacked backgrounds. Open histograms are W' signals added to the background with masses indicated in parentheses in the legend. The signal and other background samples are normalised using the integrated luminosity of the data and the NNLO (near-NNLO for $t\bar{t}$) cross sections.

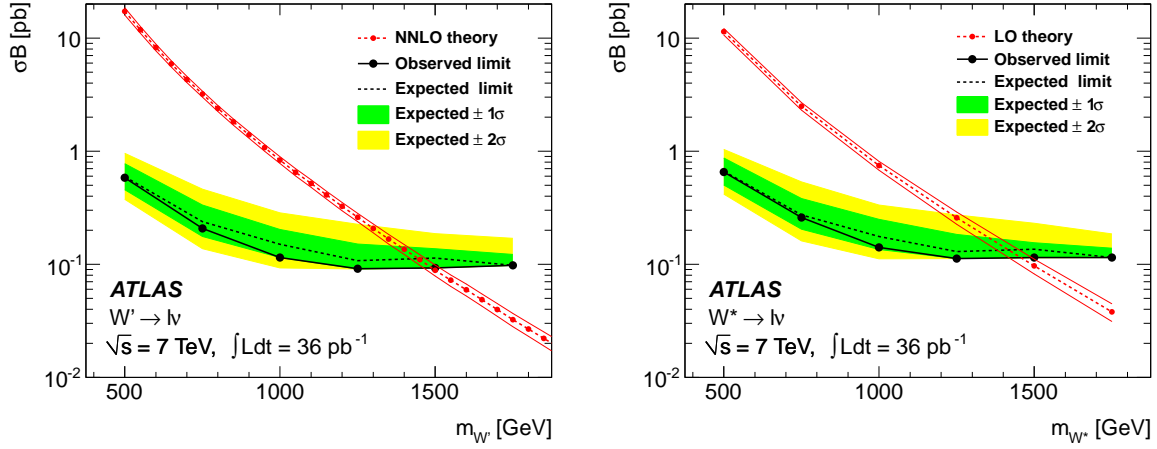


Figure 13: Limits at the 95% C.L. for W' (left) and W^* (right) production in the combination of decay channels. The solid lines show the observed limits with all uncertainties. The expected limit is indicated with dashed lines surrounded by 1σ and 2σ shaded bands. Dashed lines show the theory predictions (NNLO for W' , LO for W^*) between solid lines indicating their uncertainties.

resonance has a narrow intrinsic width compared to the detector mass resolution, and required $E_T > 25$ GeV for the electrons in the dielectron channel, and $p_T > 25$ GeV for the muons in the dimuon channel. Figure 14 shows the invariant mass distributions for the two decay channels.

Given the absence of a signal, an upper limit on the number of Z' events is determined using a Bayesian approach. For each Z' pole mass, a uniform prior in the Z' cross section was used. Figure 15 shows the limits on cross section times branching ratio for the combined decay channels. The measured and expected (shown in parenthesis) lower mass limits are 0.957 (0.964) TeV in the dielectron, 0.834 (0.895) TeV in the dimuon, and 1.048 (1.084) TeV in the combined decay channels. The lower mass limits on the E_6 gauge bosons range from 0.738 TeV (Z'_ψ) to 0.900 TeV (Z'_χ).

References

1. The ATLAS Collaboration, G. Aad *et al.*, “Search for Massive Long-lived Highly Ionising Particles with the ATLAS Detector at the LHC,” accepted by Phys. Lett. B (2011),

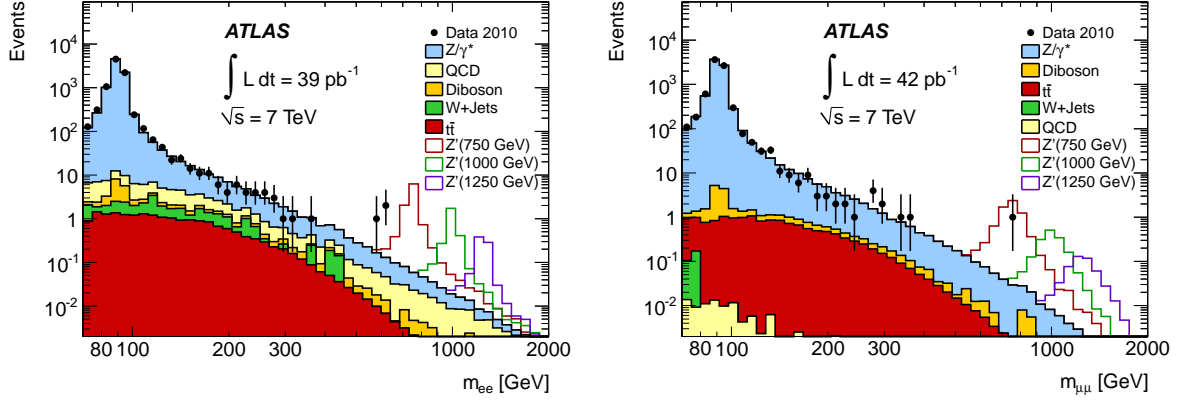


Figure 14: Dielectron (left) and dimuon (right) invariant mass distribution after final selection, compared to the stacked sum of all expected backgrounds, with three example Z'_{SSM} signals overlaid.

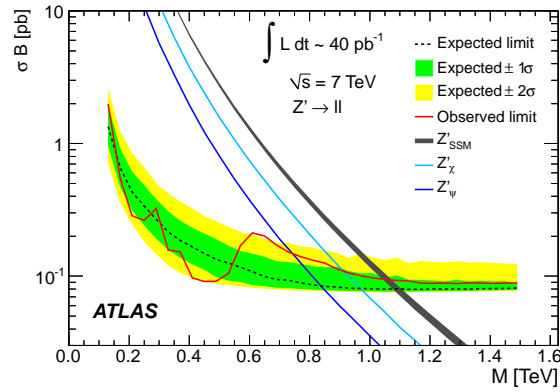


Figure 15: Expected and observed 95% C.L. limits on σB and expected σB for Z'_{SSM} production and two E_6 motivated Z' models with lowest and highest σB for the combined electron and muon channels. The thickness of the SSM curve represents the theoretical uncertainty.

CERN-PH-EP-2011-010, arXiv:1102.0459 [hep-ex].

2. The ATLAS Collaboration, G. Aad *et al.*, “Search for Diphoton Events with Large Missing Transverse Energy in 7 TeV Proton-Proton Collisions with the ATLAS Detector,” Phys. Rev. Lett. 121803 (2011).
3. The ATLAS Collaboration, G. Aad *et al.*, “Search for New Physics in Dijet Mass and Angular Distributions in pp Collisions at $\sqrt{s} = 7$ TeV Measured with the ATLAS Detector,” accepted by the New Journal of Physics (2011); CERN-PH-EP-2011-030, arXiv:1103.3864 [hep-ex].
4. The ATLAS Collaboration, G. Aad *et al.*, “Search for high-mass states with one lepton plus missing transverse momentum in proton-proton collisions at $\sqrt{s} = 7$ TeV with the ATLAS detector,” submitted to Phys. Lett. B; CERN-PH-EP-2011-023, arXiv:1103.1391 [hep-ex].
5. The ATLAS Collaboration, G. Aad *et al.*, “Search for high mass dilepton resonances in pp collisions at $\sqrt{s} = 7$ TeV with the ATLAS experiment,” submitted to Phys. Lett. B; CERN-PH-EP-2011-037, arXiv:1103.6218 [hep-ex].